Ergodic Capacity Analysis of Downlink Distributed Antenna Systems Using Stochastic Geometry

Yicheng Lin and Wei Yu
Department of Electrical and Computer Engineering
University of Toronto, Toronto, Ontario, Canada
Email: {ylin, weiyu}@comm.utoronto.ca

***Abstract*—This paper studies the ergodic capacity of a multicell distributed antenna system (DAS), where remote antenna ports are spread within each cell to cooperatively transmit to user terminals. Unlike most prior studies which assume the antenna ports to be deployed at fixed locations, this paper assumes the antenna ports to be distributed as a spatial Poisson point process (PPP) to account for the fact that in practice the antenna ports are randomly placed to cover wherever the dead spots are. We first model DAS within each cell as a downlink multiple-input single-output (MISO) channel with per-antenna power constraint while accounting for inter-cell (inter-cluster) interference. Two DAS layouts are considered: the "regular" layout where the antenna ports are randomly deployed within regular cellular boundary to serve a given user, and the "user-centric" layout where the antenna ports are distributed over a wide area and the users choose the surrounding antenna ports to form a "virtual cell" as its own serving antenna subset. Using the tool of stochastic geometry, we analytically derive efficiently computable ergodic capacity expressions for the two layouts of DAS. Using these expressions, the cell-edge capacity of DAS under the regular layout is shown to be upper-bounded by $\frac{\alpha}{2}$, where α is the pathloss exponent. Numerical results show that the proposed analytical model can accurately model the first layout, and can well approximate the second layout when the serving radius of users is not large. Compared to the traditional cellular system where all antennas are co-located at the cell center, DAS has better cell-edge performance. Further, the user-centric DAS has higher capacity than the DAS under regular layout.**

I. Introduction

Distributed antenna system (DAS) is a promising future technology for improving coverage and capacity of wireless cellular networks. By deploying remote antenna ports in coverage holes and connecting them with the home base-stations via dedicated high-speed backhaul links, DAS can cooperatively transmit to user terminals, thereby effectively mitigating detrimental effects such as shadowing and indoor penetration loss [1]. The information theoretical ergodic capacity of DAS has been studied in some recent works. The authors in [2] show that DAS can significantly improve capacity, particularly for users near cell boundaries. The capacity distributions under different number of cooperating antennas are compared in [3]. A placement optimization scheme for DAS is developed in [4] based on the ergodic capacity and the stochastic approximation theory. Uplink capacity is analyzed in [5] and [6], which show that DAS yields a much higher capacity than traditional cellular systems. However, these studies either ignore the inter-cell interference or simply assume it to be Gaussian. Explicitly modeled out-of-cell interference is included in [7], where the MIMO capacity of DAS under zero-forcing beamforming over all or a subset of antennas is evaluated.

The above studies on the capacity of DAS are all based on the assumption that antennas ports are deployed at fixed locations, e.g., uniformly on concentric circles. However, practical remote antennas may be placed at arbitrary locations to cover the dead spots, which can be modeled as a spatial random process from a birds-eye view of the network. To account for the randomness in the topology of DAS, this paper models the antenna ports as a Poisson point process (PPP) with a certain intensity. This model makes the analysis tractable by utilizing the theoretical results of stochastic geometry [8], [9]. Prior studies have used this model to analyze the capacity of multihop networks [10], traditional cellular networks [11], cellular networks with fractional frequency reuse [12], and heterogeneous networks [13], [14]. Stochastic geometry has also been applied to the analysis of DAS in [15] in deriving the outage probability as a function of the number of antennas.

This paper derives a general downlink ergodic capacity formula for DAS using stochastic geometry to enable numerical computation without Monte Carlo simulation. We explicitly model desired signals as well as inter-cell (inter-cluster) interferences. For DAS where antenna ports are randomly spread but within regular cellular boundary, we express the ergodic capacity as a function of the distance between the user and the cell center, and derive a cell-edge capacity upper bound which solely depends on the pathloss exponent. Then we apply the proposed model to the idea of "virtual cell" as introduced in [5], where users choose surrounding antennas dynamically to form its serving subset. This user-centric DAS layout eliminates the cell-edge effect and provides uniform performance for all users, at the cost of more complex backhaul management. This paper analyzes the capacity of user-centric layout under different user serving radii. Further, we compare the performance of these two layouts as well as that of the traditional cellular system. Finally, the fully distributed DAS (one antenna per port) and the partially distributed DAS (multiple antennas grouped at one port) are compared under the proposed model while fixing the total number of antennas.

II. Ergodic Capacity of DAS

This paper assumes that each user is equipped with a single antenna. Consequently, the link from the distributed

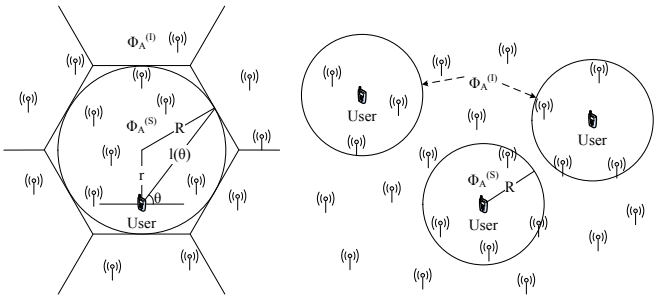

(a) (b)

Fig. 1. DAS topology. (a) Regular layout. (b) User-centric layout.

antennas within the cell to the considered user is modeled as a multiple-input single-output (MISO) channel. Since distributed antennas are physically separated, separate rather than joint power constraint should be imposed. In [16], ergodic MISO capacity with per-antenna power constraint is proved to be the same as the ergodic independent multiple-access capacity. e.g., each antenna sends independent signals with constrained power. Assuming Gaussian signaling and treating interference as noise, the ergodic capacity (in nats/s/Hz) of DAS for the user in cell o (or cluster o) is

$$\mathcal{C}=\mathbb{E}_{\mathbf{h}}\left[\ln\left(1+\frac{\sum_n P_n^{(o)}|h_n^{(o)}|^2\{r_n^{(o)}\}^{-\alpha}}{\sum_{w\neq o}\sum_m P_m^{(w)}|h_m^{(w)}|^2\{r_m^{(w)}\}^{-\alpha}+\sigma^2}\right)\right], \quad (1)$$

where n and m are the antenna indices, o and w are the cell (cluster) indices, $P_n^{(o)}$ is the transmit power of antenna n in cell (cluster) o with a fixed value μ, $h_n^{(o)}$ is the corresponding complex channel coefficient with Rayleigh distributed amplitude, $\{r_n^{(o)}\}^{-\alpha}$ models the pathloss attenuation where α is the pathloss exponent (typically $\alpha>2$), σ^2 is the noise power.

The above expectation is averaged over the channel $\mathbf{h}$ and does not take the random antenna port locations into account. We now further assume that the distributed antenna ports can be modeled as a homogeneous Poisson point process (PPP) Φ_A, and denote $\Phi_A^{(S)}$ and $\Phi_A^{(I)}$ as the subsets of points over $\mathbb{R}^2$ that consist of, respectively, antenna ports in the serving cell (cluster) o and antenna ports in all the interfering cells (clusters) $w, w\neq o$. For general partially distributed case, assume every K of the antennas are co-located within one antenna port. Let A_i be the location of antenna port i, rewrite (1) by dropping the cell (cluster) index o and w as

$$\mathcal{C}=\mathbb{E}_{\Phi_A,\mathbf{g}}\left[\ln\left(1+\frac{\sum_{A_i\in\Phi_A^{(S)}}\sum_{p=1}^K g_{ip}r_i^{-\alpha}}{\sum_{A_j\in\Phi_A^{(I)}}\sum_{q=1}^K g_{jq}r_j^{-\alpha}+\sigma^2}\right)\right]. \quad (2)$$

For simplicity we let $g_{ip}=P_{ip}|h_{ip}|^2$, which is an exponential random variable with mean $P_{ip}=\mu$ to characterize the small-scale fading from antenna p in port i to the considered user. Note that the antennas at the same port have the same pathloss attenuation. The expectation is taken over both the PPP Φ_A and the channel $\mathbf{g}$.

A. DAS under Regular Layout

First we consider DAS in the conventional sense where the coverage of home base-stations are defined by the cellular boundary. Different from [11][12] where all cells are derived from Voronoi tessellation, we adopt a hybrid approach as in [17]: the serving cell is of fixed size and modeled as a circle with radius R, while the interfering cells can be arbitrary. Thus $\Phi_A^{(S)}$ and $\Phi_A^{(I)}$ are within and outside of the cell radius R, respectively, as depicted in Fig. 1(a). Let the total expected number of antennas per cell be N, the spatial intensity of the antenna ports in $\Phi_A^{(S)}$ is therefore

$$\lambda_A^{(S)}=\frac{N}{K\pi R^2}. \quad (3)$$

Assuming homogeneity, we have $\lambda_A=\lambda_A^{(S)}=\lambda_A^{(I)}$, where $\lambda_A^{(I)}$ is the intensity of the set $\Phi_A^{(I)}$.

The considered user is randomly placed in the cell. Setting its location as the origin, we have the following theorem.

Theorem: For DAS with regular cellular boundary, the downlink ergodic capacity of the user with distance $r\leq R$ from the cell center is

$$\mathcal{C}=\int_0^\infty\left\{\exp\left[\frac{1}{2}\lambda_A(\mu s)^{2/\alpha}\int_0^{2\pi}\int_{\ell^2(\theta)(\mu s)^{-2/\alpha}}^\infty\beta(u)\mathrm{d}u\mathrm{d}\theta\right]-\exp\left[\pi\lambda_A(\mu s)^{2/\alpha}\int_0^\infty\beta(u)\mathrm{d}u\right]\right\}\frac{e^{-s\sigma^2}}{s}\mathrm{d}s, \quad (4)$$

where $\beta(u)<0$ has the form of

$$\beta(u)=(1+u^{-\alpha/2})^{-K}-1. \quad (5)$$

The term $\ell(\theta)$ in (4) is the distance from the user to the cell edge as a function of the angle θ, distance r and cell radius R, as shown in Fig. 1(a). Specifically,

$$\ell(\theta)=\sqrt{R^2-r^2\cos^2\theta}+r\sin\theta. \quad (6)$$

Proof: The derivation of the ergodic capacity of DAS with regular layout is shown in (7) on top of next page, where (a) follows from Lemma 1 in [18]:

$$\ln(1+x)=\int_0^\infty\frac{e^{-z}}{z}\left(1-e^{-xz}\right)\mathrm{d}z, \quad (8)$$

and (b) follows from a change of variable $z=s\left(\sum_{j\in\Phi_A^{(I)}}\sum_{q=1}^K g_{jq}r_j^{-\alpha}+\sigma^2\right)$. The expectation and integration are interchanged in (c) by applying the Fubini theorem (since the integrand is non-negative), and by recognizing that the subsets $\Phi_A^{(S)}$ and $\Phi_A^{(I)}$ are disjoint. In (d) we use the i.i.d. property of the fading channels among antenna ports and their independence from the PPP Φ_A; and (e) results from the fact that the sum of K independent exponential random variables with mean μ follows Erlang-K distribution with probability density function (PDF)

$$f_{\sum g}(x;K,\mu)=\frac{x^{K-1}e^{-x/\mu}}{\mu^K(K-1)!}, \quad (9)$$

$$\mathcal{C} \overset{(a)}{=} \mathbb{E}_{\Phi_A,\mathbf{g}}\left\{\int_0^\infty \frac{e^{-z}}{z}\left[1-\exp\left(\frac{-z\sum_{A_i\in\Phi_A^{(S)}}\sum_{p=1}^{K} g_{ip} r_i^{-\alpha}}{\sum_{A_j\in\Phi_A^{(I)}}\sum_{q=1}^{K} g_{jq} r_j^{-\alpha}+\sigma^2}\right)\right]\mathrm{d}z\right\} \tag{7a}$$

$$\overset{(b)}{=} \mathbb{E}_{\Phi_A,\mathbf{g}}\left\{\int_0^\infty \frac{e^{-s\sigma^2}}{s}\exp\left(-s\sum_{A_j\in\Phi_A^{(I)}}\sum_{q=1}^{K} g_{jq} r_j^{-\alpha}\right)\left[1-\exp\left(-s\sum_{A_i\in\Phi_A^{(S)}}\sum_{p=1}^{K} g_{ip} r_i^{-\alpha}\right)\right]\mathrm{d}s\right\} \tag{7b}$$

$$\overset{(c)}{=} \int_0^\infty \frac{e^{-s\sigma^2}}{s}\mathbb{E}_{\Phi_A,\mathbf{g}}\left[\exp\left(-s\sum_{A_j\in\Phi_A^{(I)}}\sum_{q=1}^{K} g_{jq} r_j^{-\alpha}\right)\right]\left\{1-\mathbb{E}_{\Phi_A,\mathbf{g}}\left[\exp\left(-s\sum_{A_i\in\Phi_A^{(S)}}\sum_{p=1}^{K} g_{ip} r_i^{-\alpha}\right)\right]\right\}\mathrm{d}s \tag{7c}$$

$$\overset{(d)}{=} \int_0^\infty \frac{e^{-s\sigma^2}}{s}\mathbb{E}_{\Phi_A}\left[\prod_{A_j\in\Phi_A^{(I)}}\mathbb{E}_{\mathbf{g}}\left[\exp\left(-sr_j^{-\alpha}\sum_{q=1}^{K} g_{jq}\right)\right]\right]\left\{1-\mathbb{E}_{\Phi_A}\left[\prod_{A_i\in\Phi_A^{(S)}}\mathbb{E}_{\mathbf{g}}\left[\exp\left(-sr_i^{-\alpha}\sum_{p=1}^{K} g_{ip}\right)\right]\right]\right\}\mathrm{d}s \tag{7d}$$

$$\overset{(e)}{=} \int_0^\infty \frac{e^{-s\sigma^2}}{s}\underbrace{\mathbb{E}_{\Phi_A}\left[\prod_{A_j\in\Phi_A^{(I)}}(1+\mu s r_j^{-\alpha})^{-K}\right]}_{\mathcal{G}_{\Phi_A^{(I)}}}\left\{1-\underbrace{\mathbb{E}_{\Phi_A}\left[\prod_{A_i\in\Phi_A^{(S)}}(1+\mu s r_i^{-\alpha})^{-K}\right]}_{\mathcal{G}_{\Phi_A^{(S)}}}\right\}\mathrm{d}s \tag{7e}$$

$$\overset{(f)}{=} \int_0^\infty \frac{e^{-s\sigma^2}}{s}\exp\left[\lambda_A\int_0^{2\pi}\int_{\ell(\theta)}^\infty\left[(1+\mu s v^{-\alpha})^{-K}-1\right]v\mathrm{d}v\mathrm{d}\theta\right]\left\{1-\exp\left[\lambda_A\int_0^{2\pi}\int_0^{\ell(\theta)}\left[(1+\mu s v^{-\alpha})^{-K}-1\right]v\mathrm{d}v\mathrm{d}\theta\right]\right\}\mathrm{d}s \tag{7f}$$

$$= \int_0^\infty \frac{e^{-s\sigma^2}}{s}\left\{\exp\left[\lambda_A\int_0^{2\pi}\int_{\ell(\theta)}^\infty\left[(1+\mu s v^{-\alpha})^{-K}-1\right]v\mathrm{d}v\mathrm{d}\theta\right]-\exp\left[2\pi\lambda_A\int_0^\infty\left[(1+\mu s v^{-\alpha})^{-K}-1\right]v\mathrm{d}v\right]\right\}\mathrm{d}s. \tag{7g}$$

which simplifies to the exponential distribution when $K=1$. Therefore

$$\mathbb{E}_{\mathbf{g}}\left(e^{-sr^{-\alpha}\sum g}\right) = \int_0^\infty f_{\sum g}(x;K,\mu)e^{-sr^{-\alpha}x}\mathrm{d}x \tag{10a}$$

$$= \int_0^\infty \frac{x^{K-1}e^{-x/\mu}}{\mu^K(K-1)!}e^{-sr^{-\alpha}x}\mathrm{d}x \tag{10b}$$

$$=(1+\mu s r^{-\alpha})^{-K}\int_0^\infty \frac{x^{K-1}e^{-\left(sr^{-\alpha}+1/\mu\right)x}}{\left(sr^{-\alpha}+1/\mu\right)^{-K}(K-1)!}\mathrm{d}x \tag{10c}$$

$$=(1+\mu s r^{-\alpha})^{-K}. \tag{10d}$$

Step (f) follows from the probability generating functional (p.g.fl.) [8] of a PPP Φ with intensity $\lambda(x)$ such that

$$\mathbb{E}_{\Phi}\left[\prod_{x\in\Phi} f(x)\right] = \exp\left\{\int_{\mathbb{R}^2}\left[f(x)-1\right]\lambda(x)\mathrm{d}x\right\}. \tag{11}$$

We apply (11) to both $\mathcal{G}_{\Phi_A^{(S)}}$ and $\mathcal{G}_{\Phi_A^{(I)}}$ in (7e), and convert from Cartesian to polar coordinates. By employing a change of variables $u = v^2(\mu s)^{-2/\alpha}$ in (7g) we have (4). ∎

The capacity expression (4) can be further simplified if we consider the special case of $K=1$ (corresponding to the fully distributed antenna deployment), $\alpha=4$, $\sigma^2=0$ (thus the power has no influence on the capacity and we can use $\mu=1$). In this case,

$$\mathcal{C} = \int_0^\infty \frac{1}{s}e^{-\frac{1}{2}\pi^2\lambda_A s^{1/2}}\left[e^{\frac{1}{2}\lambda_A s^{1/2}\tau(s)}-1\right]\mathrm{d}s, \tag{12}$$

where

$$\tau(s) = \int_0^{2\pi}\arctan\left[\ell^2(\theta)s^{-1/2}\right]\mathrm{d}\theta. \tag{13}$$

Fixing λ_A and r, the capacity expression (4) is an increasing function of R. (Note that in this case $\frac{N}{K}$ grows as $\mathcal{O}(R^2)$.) In addition, the capacity at the cell edge is also an increasing function of R (i.e., when $r=R$). This gives the following capacity upper bound for the cell-edge user:

Corollary: For DAS under regular layout, the downlink cell-edge ergodic capacity is upper bounded by $\frac{\alpha}{2}$.

Proof: Since capacity increases with R, we only need to consider the limiting case $r=R=\infty$, where $\ell(\theta)$ is

$$\ell(\theta)_{|r=R=\infty} = \begin{cases} 2R\sin\theta_{|R=\infty} = \infty & \theta\in[0,\pi] \quad (14a)\\ 0 & \theta\in[\pi,2\pi]. \quad (14b)\end{cases}$$

Substituting (14) into (4) and ignore the noise (i.e., $\sigma^2=0$), after some manipulations, the cell-edge ergodic capacity is upper bounded by

$$\mathcal{C}_{r=R}^U = \int_0^\infty \frac{1}{s}\left(e^{-Ds^{2/\alpha}}-e^{-2Ds^{2/\alpha}}\right)\mathrm{d}s \tag{15a}$$

$$\overset{(a)}{=} \frac{\alpha}{2}\int_0^\infty \frac{e^{-Dt}}{t}\left(1-e^{-Dt}\right)\mathrm{d}t \tag{15b}$$

$$\overset{(b)}{=} \frac{\alpha}{2}\ln(1+1) \tag{15c}$$

$$= \frac{\alpha}{2}\ln(2)\ \text{nats/s/Hz} = \frac{\alpha}{2}\ \text{bit/s/Hz}, \tag{15d}$$

where $D = \frac{1}{2}\pi\lambda_A\mu^{2/\alpha}\int_0^\infty\beta(u)\mathrm{d}u$, (a) follows from a change of variables $t=s^{2/\alpha}$, and (b) follows from (8). ∎

The above corollary shows that the cell-edge ergodic capacity has a limit which is solely determined by the pathloss exponent and is not a function of the antenna port density. In such a limit, the cell boundary is locally a straight line, with the serving and interfering antenna ports on each half-plane.

B. DAS under User-Centric Layout

We turn to an alternative model in which users are randomly distributed as a PPP Φ_U with intensity λ_U, superpositioned on the antenna process Φ_A, such that $\lambda_U < \lambda_A$. A user with location x forms a disc $b(x,R) = \{y \in \mathbb{R}^2 : |y-x| \le R\}$, within which the antennas are activated to serve that user. Antennas outside any disc $b(x,R)$ over $\mathbb{R}^2$ are not transmitting. The activated antenna ports can be thought of as a clustered process: start with a parent point process Φ_U formed by the users, and replace each point $x \in \Phi_U$ by a finite set of points $\Phi_A^{(x)}$ within $b(x,R)$, which is the cluster associated with x. The superposition of all clusters yields the complete process $\Phi = \bigcup_{x\in\Phi_U} \Phi_A^{(x)}$. The topology is shown in Fig. 1(b).

To assure quality of service, we assume that the communicating users do not have overlapping serving areas, i.e., the minimum distance between any two neighboring users is $2R$. This can be achieved by proper user scheduling. The daughter points in the representative clusters are PPP with intensity λ_A.

The derivation of the user ergodic capacity in the user-centric layout differs from that of the regular DAS layout in step (7e) in the computations of $\mathcal{G}_{\Phi_A^{(S)}}$ and $\mathcal{G}_{\Phi_A^{(I)}}$. Assume the considered user is at the origin, then $\Phi_A^{(S)} = \Phi_A^{(0)}$ is a PPP with intensity λ_A within the disc $b(0,R)$. Using (11) we have

$$\mathcal{G}_{\Phi_A^{(S)}} = \exp\left\{2\pi\lambda_A \int_0^R \left[(1+\mu s v^{-\alpha})^{-K} - 1\right] v \mathrm{d}v\right\}. \quad (16)$$

Since only the activated antennas within each $b(x,R), |x| \ge 2R$ contribute as interferences, $\Phi_A^{(I)} = \bigcup_{x\in\Phi_U\setminus\{0\}} \Phi_A^{(x)}$ is a clustered process. However, the parent points of the clusters are not Poisson but the hard-core process with a repel distance ($2R$ in our case). The p.g.fl. of this process is in general mathematically formidable. However, we can use the PPP to approximate the hard-core process of the parent points within a bounded excess interference ratio relative to Poisson, as discussed in [19] for the type II Matérn hard-core process. The compound clustered process, therefore, can be approximated by the Poisson clustered process (PCP) since both the parent and daughter points are now PPP. The p.g.fl. is [8][20]:

$$\mathbb{E}_\Phi\left[\prod\nolimits_{x\in\Phi} f(x)\right] = \exp\left\{\int_{\mathbb{R}^2} \left[\mathcal{M}\left[f(x)\right] - 1\right] \lambda_p(x) \mathrm{d}x\right\}, \quad (17)$$

where $\lambda_p(x)$ is the intensity of the parent PPP and

$$\mathcal{M}\left[f(x)\right] = \exp\left\{\bar{c}\left[\int_{\mathbb{R}^2} f(x+y)\delta(y)\mathrm{d}y - 1\right]\right\}, \quad (18)$$

where $\bar{c}$ is the average number of points within each representative daughter cluster, and $\delta(y)$ is the probability density function of the daughter cluster. In this case $\bar{c}$ is the number of serving antenna ports per user $\bar{c} = \lambda_A \pi R^2$, and since antenna ports are uniformly distributed over $b(x,R)$ in 2-dimensional Poisson model, we have $\delta(y) = 1/\pi R^2$ for $||y|| \le R$.

Applying (17) to $\mathcal{G}_{\Phi_A^{(I)}}$ in (7e) and plugging in $\bar{c}$ and $\delta(y)$, after some manipulations we have

$$\mathcal{G}_{\Phi_A^{(I)}} = \exp\left\{\lambda_U \int_0^{2\pi}\int_{2R}^{\infty} \left[\exp\left[\lambda_A H\left(s,v,\theta\right)\right] - 1\right] v \mathrm{d}v \mathrm{d}\theta\right\}, \quad (19)$$

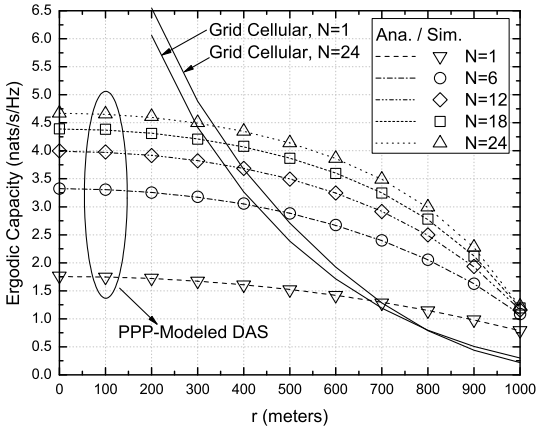

Fig. 2. Grid cellular vs. PPP-modeled DAS with regular layout: ergodic capacity as a function of cell center to user distance r and antenna intensity (antenna number per cell N). $\alpha = 4$, $K = 1$, $R = 1000$.

where the integration limits of v are from $2R$ to ∞ because the closest parent point (one of other users) is at a distance at least $2R$. The term $H\left(s,v,\theta\right)$ in (19) is defined as

$$H\left(s,v,\theta\right) = \int_0^{2\pi}\int_0^R (1+\mu s \rho^{-\alpha})^{-K} u \mathrm{d}u \mathrm{d}\xi - \pi R^2, \quad (20)$$

where ρ is the distance from an antenna port in an interfering cluster to the user under consideration, which satisfies

$$\rho^2 = u^2 + v^2 + 2uv\cos(\theta - \xi). \quad (21)$$

Since θ in (19) only appears in $\cos(\theta - \xi)$ in the expression for ρ, using the symmetry of the $\cos(\cdot)$ function, (19)-(21) can be further simplified by removing the θ variable

$$\mathcal{G}_{\Phi_A^{(I)}} = \exp\left\{2\pi\lambda_U \int_{2R}^{\infty} \left[\exp\left[\lambda_A H\left(s,v\right)\right] - 1\right] v \mathrm{d}v\right\}, \quad (22)$$

where $H\left(s,v,\theta\right)$ is reduced to $H\left(s,v\right)$ since

$$\rho^2 = u^2 + v^2 + 2uv\cos\xi. \quad (23)$$

Substituting (16) and (22) into (7e), we have the following proposition.

Proposition: For DAS under user-centric layout, the downlink user ergodic capacity can be approximated by

$$\mathcal{C} \approx \int_0^\infty \frac{e^{-s\sigma^2}}{s} \exp\left[2\pi\lambda_U \int_{2R}^{\infty} \left[\exp\left[\lambda_A H\left(s,v\right)\right] - 1\right] v \mathrm{d}v\right] \times \left\{1 - \exp\left[2\pi\lambda_A \int_0^R \left[(1+\mu s v^{-\alpha})^{-K} - 1\right] v \mathrm{d}v\right]\right\} \mathrm{d}s, \quad (24)$$

where $H\left(s,v\right)$ is the same as in (20), but with ρ from (23).

III. Numerical Results

We present numerical simulations to verify our theoretical results. First we demonstrate the ergodic capacity of DAS under regular layout. The total per-cell power is $P = 46$dBm, which is evenly divided among antennas in the cell, i.e., $P_n = \frac{P}{N}$. We set the cell radius to $R = 1000$m and vary the user-to-cell-center distance r. Compared with the Monte Carlo

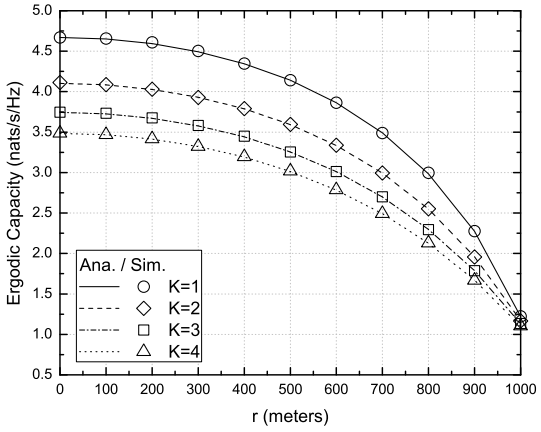

Fig. 3. DAS with regular layout: ergodic capacity as a function of cell center to user distance r and antenna number per antenna port K. $\alpha = 4$, $N = 24$, $R = 1000$. The number of antenna ports is $\frac{N}{K}$.

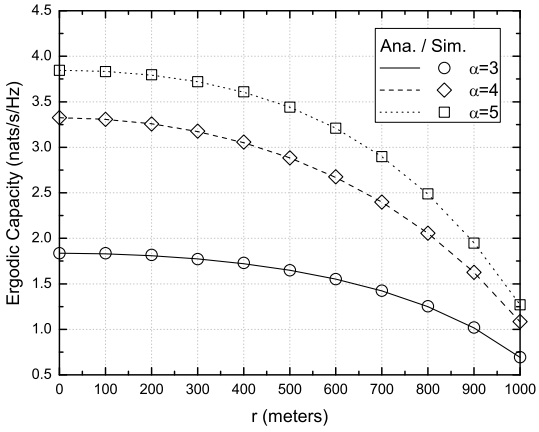

Fig. 4. DAS with regular layout: ergodic capacity as a function of cell center to user distance r and pathloss exponent α. $N = 6$, $K = 1$, $R = 1000$.

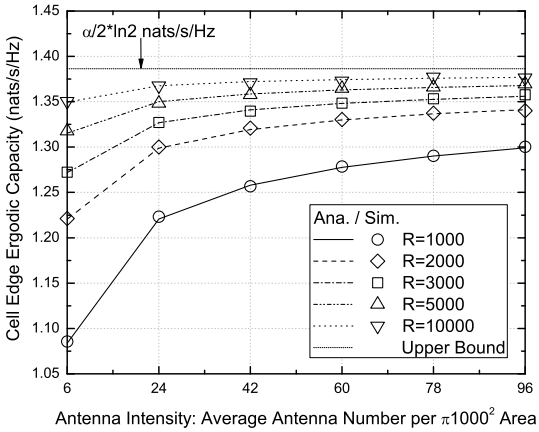

Fig. 5. DAS with regular layout: cell-edge ergodic capacity as a function of antenna intensity (average antenna number per $\pi 1000^2$ area) and cell radius R. $\alpha = 4$, $K = 1$, $r = R$.

experiments, the analytical integrations can be computed more efficiently, and its effectiveness is verified with simulation as shown in Fig. 2. Note that the ergodic capacity drops from the cell center to the cell edge, and with a stochastic-geometry-based analysis there is no such "rise-and-drop" effect for capacity as observed in [2][7] for fixed deployment, i.e., when user approaches a fixed-location antenna the capacity rises, and drops otherwise. The simulated results for cellular systems where all antennas are co-located at the cell center are depicted as "Grid Cellular" in Fig. 2. As compared to DAS, the capacity of the centralized cellular architecture is higher in the cell center but deteriorates at the cell edge, which reflects DAS's ability in achieving ubiquitous coverage. Another observation from Fig. 2 is that the gap between $N = 1$ and $N = 24$ is much more significant for DAS than for the co-located one. This is because unlike the latter layout, more antennas in DAS means statistically shorter distance between a user and its closest serving antenna port, and thus much higher capacity. In Fig. 3, we fix the total number of the antennas and vary the number of antennas per port, and show that the fully distributed case ($K = 1$) outperforms partially distributed case ($K > 1$). Fig. 4 shows that greater pathloss exponent leads to larger capacity, since interferences drop faster than the desired signal with the rise of the attenuation. We further confirm our cell-edge capacity upper bound in Fig. 5, the capacity increases with the antenna intensity and cell radius, but is always upper bounded by $2 \ln 2$ nats/s/Hz when $\alpha = 4$.

For DAS under user-centric layout, we assume the equivalent network parameters as that of the regular DAS layout with cell radius of 1000m for fair comparison. The average number of users over an area of $\pi 1000^2$ is one, i.e., $\lambda_U = \frac{1}{\pi 1000^2}$. The antenna port intensity is $\lambda_A = \frac{N}{K\pi 1000^2}$, and the average sum power over an area of $\pi 1000^2$ is $P = 46$dBm, which is equally shared by all antennas within the area. For the simulation, we adopt the Simple Sequential Inhibition (SSI) model [21] to represent the hard-core process. Specifically, we generate users with a specified intensity in a sequential manner; add a random new user to the network only if its distance to any of the previous added users is greater than $2R$. We vary the user's serving radius R for the analytical and the simulated results. Note that the maximum R of the simulated results is only 700m, since the hard-core process of the users reaches saturation for R greater than this value and no further active users can be added. In Fig. 6, it is observed that the analytical results match the simulated ones when $R \leq 400$, but deviate from the simulation at $R > 400$. It is because the collision probability of a newly generated user with the existing ones is the complement of the void probability of PPP

$$\mathbb{P}_{\text{colli.}} = 1 - \mathbb{P}\left(\text{No other users within a radius of } 2R\right) \quad (25a)$$

$$= 1 - e^{-4\lambda_U \pi R^2}. \quad (25b)$$

At a smaller serving radius R, the collision probability is low, thus the SSI model used for the parent point process is close to the Poisson model, and the clustered process can be well approximated by PCP. Such approximation is not accurate when R gets larger, and the analytical capacity is higher than the simulated one. This is because the Poisson process, as

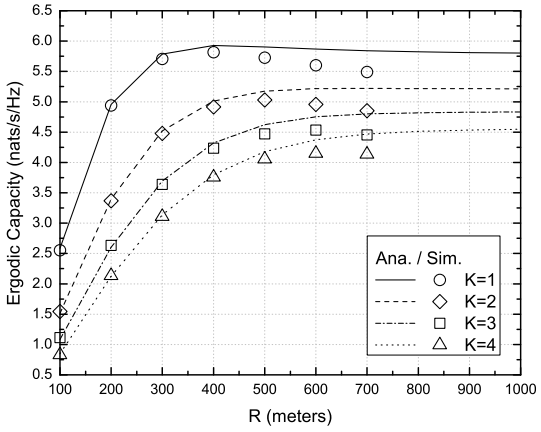

Fig. 6. DAS with user-centric layout: ergodic capacity as a function of user serving radius R and antenna number per antenna port K. $\alpha = 4$, $N = 24$.

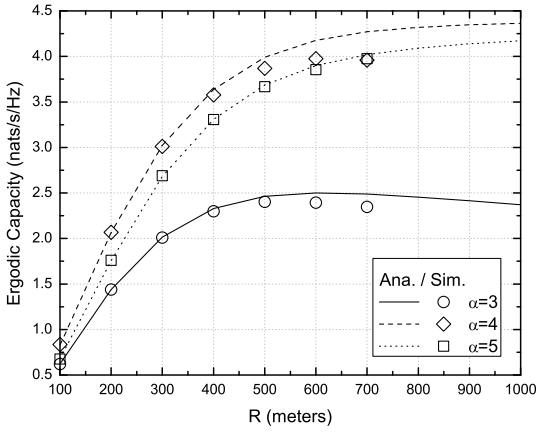

Fig. 7. DAS with user-centric layout: ergodic capacity as a function of user serving radius R and pathloss exponent α. $N = 6$, $K = 1$.

we assumed for the user distribution in analysis, yields less interference than that of the hard-core process of the same density [19]. In Fig. 7, we vary the pathloss exponent and find that the maximum capacity is achieved when $\alpha = 4$ instead of $\alpha = 5$, which is different from Fig. 4. This is counter-intuitive and shows one difference between the regular and the user-centric layout. In particular, the analytical result is very close to the Monte Carlo result under $\alpha = 5$. It is also worth to note, as observed in Fig. 6 and Fig. 7, that capacity is not a monotonic function of R in some cases.

Compare the two different DAS layouts (e.g., Fig. 3 vs. Fig. 6, Fig. 4 vs. Fig. 7), the user-centric layout has a higher maximum capacity than the regular layout even when the user of the latter is in the cell center. This is because only the antennas close to active users are transmitting in the user-centric layout, which avoids extra interference. However, the user-centric DAS faces challenges such as dynamic backhaul management as users' antenna sets may change over time, and scheduling issues as how to choose non-conflicting users.

IV. Conclusion

In this paper, the downlink ergodic capacity of DAS is derived in a tractable form by modeling the antennas as a Poisson point process. We present the capacity results of DAS under two different layouts, and demonstrate the effectiveness of the proposed analytical model. Results show that DAS achieves better cell-edge capacity than the cellular system, and the user-centric DAS has higher maximum capacity over the DAS with regular cellular boundary.

References

[1] K. Kerpez, "A radio access system with distributed antennas," *IEEE Trans. Veh. Technol.*, vol. 45, no. 2, pp. 265–275, May 1996.

[2] W. Choi and J. Andrews, "Downlink performance and capacity of distributed antenna systems in a multicell environment," *IEEE Trans. Wireless Commun.*, vol. 6, no. 1, pp. 69–73, Jan. 2007.

[3] J. Park, E. Song, and W. Sung, "Capacity analysis for distributed antenna systems using cooperative transmission schemes in fading channels," *IEEE Trans. Wireless Commun.*, vol. 8, no. 2, pp. 586–592, Feb. 2009.

[4] S. Firouzabadi and A. Goldsmith, "Downlink performance and capacity of distributed antenna systems." [Online]. Available: arXiv:1109.2957

[5] L. Dai, S. Zhou, and Y. Yao, "Capacity analysis in CDMA distributed antenna systems," *IEEE Trans. Wireless Commun.*, vol. 4, no. 6, pp. 2613–2620, Nov. 2005.

[6] L. Dai, "A comparative study on uplink sum capacity with co-located and distributed antennas," *IEEE J. Sel. Areas Commun.*, vol. 29, no. 6, pp. 1200–1213, June 2011.

[7] R. Heath, T. Wu, Y. Kwon, and A. Soong, "Multiuser MIMO in distributed antenna systems with out-of-cell interference," *IEEE Trans. Signal Process.*, vol. 59, no. 10, pp. 4885–4899, Oct. 2011.

[8] M. Haenggi, *Stochastic Geometry for Wireless Networks*. Cambridge University Press, 2012.

[9] M. Haenggi, J. Andrews, F. Baccelli, O. Dousse, and M. Franceschetti, "Stochastic geometry and random graphs for the analysis and design of wireless networks," *IEEE J. Sel. Areas Commun.*, vol. 27, no. 7, pp. 1029–1046, Sept. 2009.

[10] J. Andrews, S. Weber, M. Kountouris, and M. Haenggi, "Random access transport capacity," *IEEE Trans. Wireless Commun.*, vol. 9, no. 6, pp. 2101–2111, June 2010.

[11] J. Andrews, F. Baccelli, and R. Ganti, "A tractable approach to coverage and rate in cellular networks," *IEEE Trans. Commun.*, vol. 59, no. 11, pp. 3122–3134, Nov. 2011.

[12] T. Novlan, R. Ganti, A. Ghosh, and J. Andrews, "Analytical evaluation of fractional frequency reuse for OFDMA cellular networks," *IEEE Trans. Wireless Commun.*, vol. 10, no. 12, pp. 4294–4305, Dec. 2011.

[13] H. Dhillon, R. Ganti, F. Baccelli, and J. Andrews, "Modeling and analysis of K-tier downlink heterogeneous cellular networks," *IEEE J. Sel. Areas Commun.*, vol. 30, no. 3, pp. 550–560, Apr. 2012.

[14] H. Jo, Y. Sang, P. Xia, and J. Andrews, "Heterogeneous cellular networks with flexible cell association: A comprehensive downlink SINR analysis," *IEEE Trans. Wireless Commun.*, vol. 11, no. 10, pp. 3484–3495, Oct. 2012.

[15] J. Zhang and J. Andrews, "Distributed antenna systems with randomness," *IEEE Trans. Wireless Commun.*, vol. 7, no. 9, pp. 3636–3646, Sept. 2008.

[16] M. Vu, "MISO capacity with per-antenna power constraint," *IEEE Trans. Commun.*, vol. 59, no. 5, pp. 1268–1274, May 2011.

[17] R. Heath and M. Kountouris, "Modeling heterogeneous network interference," in *Proc. Inf. Theory App. Workshop (ITA)*, Feb. 2012, pp. 17–22.

[18] K. Hamdi, "Capacity of MRC on correlated rician fading channels," *IEEE Trans. Commun.*, vol. 56, no. 5, pp. 708–711, May 2008.

[19] M. Haenggi, "Mean interference in hard-core wireless networks," *IEEE Commun. Lett.*, vol. 15, no. 8, pp. 792–794, Aug. 2011.

[20] R. Ganti and M. Haenggi, "Interference and outage in clustered wireless ad hoc networks," *IEEE Trans. Inf. Theory*, vol. 55, no. 9, pp. 4067–4086, Sept. 2009.

[21] A. Busson and G. Chelius, "Point processes for interference modeling in csma/ca ad-hoc networks," in *Proc. ACM Int. Symp. Perform. Eval. Wireless Ad Hoc, Sensor, and Ubiquitous Networks (PE-WASUN)*, Oct. 2009, pp. 33–40.